EEG Source Imaging based on Spatial and Temporal Graph Structures

Technical Report · September 2017

CITATIONS
0

READS
138

4 authors:

Jing Qin
Montana State University
20 PUBLICATIONS **72** CITATIONS
SEE PROFILE

Feng Liu
University of Texas at Arlington
12 PUBLICATIONS **46** CITATIONS
SEE PROFILE

Shouyi Wang
University of Texas at Arlington
36 PUBLICATIONS **167** CITATIONS
SEE PROFILE

Jay M. Rosenberger
University of Texas at Arlington
79 PUBLICATIONS **789** CITATIONS
SEE PROFILE

EEG Source Imaging based on Spatial and Temporal Graph Structures

Jing Qin[1], Feng Liu[2], Shouyi Wang[2] and Jay Rosenberger[2]
[1] Department of Mathematical Sciences, Montana State University, Bozeman, MT, USA
E-mail: jing.qin@montana.edu
[2] Department of Industrial Engineering, University of Texas at Arlington, Arlington, TX, USA
E-mail: feng.liu@mavs.uta.edu, {shouyiw,jrosenbe}@uta.edu

***Abstract*— EEG serves as an essential tool for brain source localization due to its high temporal resolution. However, inference of brain activities from the EEG data is in general a challenging ill-posed inverse problem. To better retrieve task related discriminative source patches from strong spontaneous background signals, we propose a novel EEG source imaging model based on spatial and temporal graph structures. In particular, graph fractional-order total variation (gFOTV) is used to enhance spatial smoothness, and the label information of brain state is enclosed in a temporal graph regularization term to guarantee intra-class consistency of estimated sources. The proposed model is efficiently solved by the alternating direction method of multipliers (ADMM). A two-stage algorithm is proposed as well to further improve the result. Numerical experiments have shown that our method localize source extents more effectively than the benchmark methods.**

***Keywords*— EEG Source Imaging, Graph Fractional-Order Total Variation, Graph Regularization, Alternating Direction Method of Multiplier (ADMM).**

I. Introduction

Electroencephalography (EEG) is a non-invasive brain imaging technique that records the electric field on the scalp generated by the synchronous activation of neuronal populations. It has been previously estimated that if as few as one in a thousand synapses become activated simultaneously in a region of about 40 square millimeters of cortex, the generated signal can be detected and recorded by EEG electrodes [1]. Compared to other functional neuroimaging techniques such as functional magnetic resonance imaging (fMRI) and positron emission tomography (PET), EEG is able to directly measure real-time electrical neural activities, and therefore EEG can identify exactly *when* different brain regions are involved during different processing [2]. By contrast, PET and fMRI infer brain activities by detecting associated metabolic or cerebrovascular changes which are slow and time-delayed [1], [3]. Besides, due to its easy portability, low cost and high temporal resolution, EEG has been a leading clinical tool for detecting and diagnosing brain disorders and diseases.

Reconstruction of activated brain sources from the recorded EEG data is known as the EEG inverse problem or source imaging/localization, which is highly ill-posed without a unique solution since the number of dipoles (in thousands) is much higher than that of electrodes (in hundreds). Based on different assumptions about source configurations, a variety of methods have been proposed to address this challenging problem particularly with various regularization techniques. One of the pioneering work is the ℓ_2-norm based minimum norm estimate (MNE) inverse solver [4]. By replacing ℓ_2-norm by ℓ_1-norm, minimum current estimate (MCE) [5] is proposed to overcome overestimation of active area sizes incurred by ℓ_2-norm. Pascual-Marqui et al. proposed standardized low-resolution brain electromagnetic tomography (sLORETA) [6] that enforces spatial smoothness of the neighboring sources and normalizes the solution with respect to the estimated noise level. It has been found that source extents can be well estimated by enforcing sparsity in a transformed domain, e.g., total variation (TV) regularization [7], [8] More recently, variants of TV based regularization techniques have been proposed to enhance higher order spatial smoothness, including the second-order total generalized variation based s-SMOOTH [7], and the graph fractional-order TV based EEG source localization method [9], [10].

On the other hand, considering spatial sparsity and temporal smoothness, a number of regularization techniques based on spatiotemporal mixed norms have been developed, including Mixed Norm Estimates (MxNE) which uses $\ell_{1,2}$-norm regularization [11], and time-frequency mixed-norm estimate (TF-MxNE) which uses structured sparse priors in time-frequency domain for better estimation of the non-stationary and transient source signal [12]. In fact, discriminative task-related brain activation sources are more important and useful for clinical practice. According to our recent work on discovering discriminative source activations [13]–[15], EEG label information of brain state such as happiness, sadness and calmness could be incorporated into the EEG inverse problem solvers in a mutually beneficial manner. In this paper, we propose a novel EEG source imaging model based on spatial-temporal graph structures by exploiting label information of brain state. In particular, the graph fractional-order TV is used for preserving high-order spatial smoothness and the temporal graph regularization promotes intra-class consistency. The proposed model is solved by a two-stage algorithm based on the alternating direction method of multipliers (ADMM) and geolocation-based solution expansion, which avoids the risk of getting stuck in undesirable suboptimal solutions. Numerical experiments are conducted to verify the effectiveness of the proposed work on discovering discriminative source extents.

The rest of the paper is organized as follows. Section

II introduces the EEG inverse problem. Section III reviews the spatial graph fractional-order TV and the temporal graph regularization. Section IV describes the proposed approach together with its numerical algorithm in detail. Section V evaluates the proposed work numerically. A brief conclusion is drawn in Section VI.

II. Inverse Problem

EEG data are mostly generated by pyramidal cells in the gray matter with an orientation perpendicular to the cortex. It is well-established that the orientation of a brain source is perpendicular to the cortex surface. Assume that there are N EEG electrodes on the scalp for measuring T time samples. Consider a cortex with D triangles or dipoles. Let $L \in \mathbb{R}^{N\times D}$ be the *lead field matrix* that describes the superposition of linear mappings from the cortex sources to the EEG recording sensors, each column of which represents the electrical potential mapping pattern of a cortex dipole to the EEG electrodes. In the noise-free case, the forward model can be expressed as

$$X = LS, \tag{1}$$

where $X \in \mathbb{R}^{N\times T}$ is the EEG measurements. Here $S \in \mathbb{R}^{D\times T}$ represents the electrical potentials in D source locations for all the T time points that is transmitted to the scalp surface. Since L has much more columns than rows, the inverse problem that retrieving S from X becomes highly ill-posed. In order to find a unique solution, we resort to a regularization technique by introducing prior information of the solution. More specifically, S can be obtained by solving the following minimization problem

$$\min_S \|X - LS\|_F^2 + \lambda R(S), \tag{2}$$

where $\|\cdot\|_F$ is the Frobenius norm of a matrix. The first term of (2) is called *data fidelity* which accounts for the prediction error, and the second term is called *regularization* term which usually corresponds to certain characteristics of the solution, e.g., the sparsity by itself or in some transformed domain. Selection of the regularization term plays a key role in the source imaging and discriminative source patch classification. To improve the localization accuracy, $R(S)$ is chosen to encourage spatially smooth source configurations and enforce neurophysiologically plausible solutions.

III. Spatial and Temporal Graph Regularizations

In this section, we briefly review the spatial graph fractional-order TV, and the temporal graph regularization involving the label information of different brain states.

A. Spatial Graph Fractional-Order Total Variation

In pursuit of improving spatial smoothness of source extents, we design a spatial regularization term based on our recent work on graph fractional-order TV [9]. To reduce staircase artifacts of TV, fractional-order TV (also known as total fractional-order variation) has been proposed and widely applied in the image processing community to improve image smoothness by considering more neighboring information [16]–[18]. It is known that the anisotropic fractional-order TV of an image u defined on a 2D rectangular mesh has the following form

$$TV_\alpha(u) = \|\nabla^\alpha u\|_1 = \sum_{i,j=1}^{M} \big(|(D_x^\alpha u)_{i,j}| + |(D_y^\alpha u)_{i,j}|\big),$$

where $\alpha \in (1, 2)$. Here the fractional derivative is based on the Grüwald-Letnikov derivative definition [19]

$$(D_x^\alpha u)_{i,j} = \sum_{k=0}^{K} w_\alpha(k) u(i-k, j),$$
$$(D_y^\alpha u)_{i,j} = \sum_{k=0}^{K} w_\alpha(k) u(i, j-k),$$

where the coefficients are $w_\alpha(k) = (-1)^k \frac{\Gamma(\alpha+1)}{k!\Gamma(\alpha-k+1)}$. Based on this definition, TV_α becomes the traditional TV when $\alpha = 1$. Although valid for $(0, 1) \cup (2, \infty)$, the parameter α is typically set between 1 and 2 to achieve the best performance in practice [17].

Using a triangle mesh, the discretized cortex surface can be treated as a graph with voxel or dipole as graph node. For a specific node v_i, let $d(v_i, v_j)$ be the number of nodes on the shortest path connecting the nodes v_i and v_j, which is in or close to a geodesic of the underlying cortex surface passing through v_i and v_j. Given a path $p = (v_{i=m_0}, v_{m_1}, \ldots, v_{m_K})$ where the shortest distance between v_{m_0} and v_{m_j} is j nodes, the fractional-order derivative along the path p is defined as

$$(D_p^\alpha u)_i := D_p^\alpha u(v_i) = \sum_{j=0}^{K} w_\alpha(j) u(v_{m_j}).$$

The discretized fractional-order TV of u is defined as [9]:

$$TV_\alpha(u) = \|D_\alpha u\|_1 = \sum_{i=1}^{M} \sum_{p\in\mathcal{P}(i;K)} |(D_p^\alpha u)_i|,$$

where $\mathcal{P}(i; K)$ is the set of all paths starting from the i-th node with length of K nodes. Here we use the breadth-first search (BFS) algorithm to first compute the shortest path between each node pair to get a pairwise distance matrix, and then create the matrix $D_\alpha \in \mathbb{R}^{N_p\times D}$ by seeking all N_p paths of length K nodes and recording all nodes on each path. For a specific node v_i, the nodes at level k, i.e., the nodes have shortest distance k from v_i, are assigned the weight $w_\alpha(k)$. Note that K specifies the maximal level of nodes to be used. By the assumption that u has a sparse spatial structure, it is sufficient to use $K \leq 4$ levels of neighboring nodes to achieve the desired accuracy in our experiments.

B. Temporal Graph Regularization

Inspired by discovering image discriminators using graph regularization in computer vision [20], we design a temporal regularization to penalize intra-class in-consistency. More

specifically, the common sources are first decomposed using the Voting Orthogonal Matching Pursuit (VOMP) algorithm [13]. Define a binary matrix M as follows

$$M_{ij} = \begin{cases} 1, & \text{if } (s_i, s_j) \text{ belong to the same class;} \\ 0, & \text{otherwise.} \end{cases}$$

It is obvious that M contains the label information of different brain state. Now define a temporal graph regularization as

$$R_t(S) = \sum_{i,j=1}^{N} \|s_i - s_j\|_2^2 M_{ij},$$

where s_i is the i-th column of the matrix S. This formulation intends to find discriminative sources by decomposing the common source while preserving consistency of reconstructed sources in the same class. By defining D as a diagonal matrix whose diagonal entries are row sums of the symmetric matrix M, i.e., $D_{ii} = \sum_j M_{ij}$, and denoting $G = D - M$, $R_t(S)$ can be rewritten as:

$$R_t(S) = \sum_{i,j=1}^{N} ({s_i}^T s_i + {s_j}^T s_j - 2{s_i}^T s_j) M_{ij} = 2\,\mathrm{tr}(SGS^T), \tag{3}$$

where $\mathrm{tr}(\cdot)$ is the trace operator of a matrix, i.e., adding up all diagonal entries of a matrix.

IV. Proposed EEG Source Imaging Approach

In this section, we present our proposed approach which utilizes the temporal and spatial graph structures of the EEG data to help recognize extended source patches on the cortex and enhance spatial smoothness of source extents. A numerical algorithm is derived by applying the ADMM and an enhanced version based on the derived algorithm called Two-stage Geolocation-based Solution Expansion ADMM (TGSE-ADMM) is proposed.

A. Proposed EEG Source Imaging Model

There has been a large number of work devoted to developing EEG source localization methods by using various regularization techniques, such as Variation-Based Sparse Cortical Current Density (VB-SCCD) [8] which is essentially the TV, In [21], Zhu et al. proposed to use multiple priors including variation-based and wavelet-based constraints. However, based on the assumption that the underlying signal is piecewise constant, TV can easily cause staircase artifacts. To preserve high-order spatial smoothness of the EEG signal defined on the cortex, we use the graph fractional-order total variation described in Section III-A. On the other hand, previous studies [22], [23] indicated that the brain spontaneous sources contribute most part of the EEG signal. The neurons in our brain still fires even when the subjects are in closed-eye resting state.

By combining the spatial and temporal graph regularizations described in Section III, we propose the following model for EEG discriminative source imaging

$$\begin{aligned} &\min_S E(S) + R_s(S) + R_t(S) \\ &= \min_S \frac{1}{2}\|X - LS\|_F^2 + \lambda\|D_\alpha S\|_{1,1} + \frac{\beta}{2}\sum_{i,j=1}^{N}\|s_i - s_j\|_2^2 M_{i,j} \end{aligned} \tag{4}$$

where $\beta, \lambda > 0$ are tuning parameters and $\|D_\alpha S\|_{1,1} = \sum_{i=1}^{T}\|D_\alpha s_i\|_1$. Note that an important assumption in EEG source imaging is the prior to guarantee spatiotemporal smoothness in the source solution [11], [24]–[27]. Our proposed model is able to enforce high order spatial smoothness via graph fractional-order TV plus temporal smoothness via temporal graph regularization involving label information of brain state.

B. Proposed Algorithms

To simplify discussion, we first replace the temporal regularization term by (3) and rewrite (4) as follows

$$\min_S \frac{1}{2}\|X - LS\|_F^2 + \lambda\|D_\alpha S\|_{1,1} + \beta(\mathrm{tr}(SGS^T)). \tag{5}$$

By change of variables, (5) can be rewritten as

$$\min_{S,Y} \frac{1}{2}\|X - LS\|_F^2 + \lambda\|Y\|_{1,1} + \beta(\mathrm{tr}(SGS^T)) \text{ s.t. } Y = D_\alpha S. \tag{6}$$

The new formulation makes the objective function separable with respect to the two variables S and Y. Furthermore, by denoting the i-th column of X and Y by x_i and y_i respectively, we obtain a column-wise form of (6)

$$\min_{s_i, y_i} \frac{1}{2}\|x_i - Ls_i\|_2^2 + \lambda\|y_i\|_1 + \beta G_{ii} s_i^T s_i + s_i^T h_i \text{ s.t. } y_i = D_\alpha s_i, \tag{7}$$

where $h_i = 2\beta(\sum_{j\neq i} G_{ij} s_j)$ and G_{ij} is the (i,j)-th entry of the matrix G.

ADMM is an efficient method to solve convex and even non-convex problems by decomposing the original problem into several subproblems such that each subproblem has a closed form solution or can be computed efficiently [28]. To apply the ADMM to solve (7), we first construct the following augmented Lagrangian function

$$\begin{aligned} \mathcal{L}(s_i, y_i, u_i) = &\frac{1}{2}\|x_i - Ls_i\|_2^2 + \lambda\|y_i\|_1 + \beta G_{ii} s_i^T s_i \\ &+ s_i^T h_i + u_i^T(D_\alpha s_i - y_i) + \frac{\rho}{2}\|D_\alpha s_i - y_i\|_2^2 \end{aligned} \tag{8}$$

Then ADMM results in the following two subproblems for updating s_i, y_i:

$$\begin{aligned} s_i^{(k+1)} &= \operatorname*{argmin}_s \mathcal{L}(s, y_i^{(k)}, u_i^{(k)}), \\ y_i^{(k+1)} &= \operatorname*{argmin}_y \mathcal{L}(s_i^{(k+1)}, y, u_i^{(k)}). \end{aligned}$$

Algorithm 1 Source Imaging Based on Spatial and Temporal Graph Structures

INPUT: Lead field matrix L, preprocessed EEG signal matrix X, graph matrix G, precalculated matrix D_α, parameters $\beta, \lambda > 0$, Homotopy solution S_0, and $\kappa > 0$.
OUTPUT: Source matrix S.
Initialize: Set $S^{(0)} = S_0$, $y_i^{(0)} = VS_0$ and $u_i^{(0)} = \kappa \times \mathbf{1}$.
for $t = 1, \ldots, T_{max}$ **do**
  for $i = 1, \ldots, N$ **do**
    while s_i is not converged **do**

$$s_i^{(k+1)} = P^{-1}[L^T x_i - h_i + \rho D_\alpha^T (y_i^{(k)} - u_i^{(k)}/\rho)],$$
$$y_i^{(k+1)} = \text{shrink}(D_\alpha s_i^{(k+1)} + u_i^{(k)}/\rho, \lambda/\rho),$$
$$u_i^{(k+1)} = u_i^{(k)} + \rho(D_\alpha s_i^{(k+1)} - y_i^{(k+1)})$$

    end while
  end for
  update S_t, Y_t
end for

The s-subproblem has a least-squares solution

$$\begin{aligned} s_i^{(k+1)} &= \underset{s}{\text{argmin}} \frac{1}{2}\|x_i - Ls\|_2^2 + \beta G_{ii} s^T s + s^T h_i \\ &\quad + \frac{\rho}{2}\|D_\alpha s - y_i^{(k)} + u_i^{(k)}/\rho\|_2^2 \\ &= P^{-1}[L^T x_i - h_i + \rho D_\alpha^T (y_i^{(k)} - u_i^{(k)}/\rho)], \end{aligned}$$

where $P = L^T L + 2\beta G_{ii} I + \rho D_\alpha^T D_\alpha$. The y-subproblem essentially finds the proximal operator of the ℓ_1-norm, which has a closed form

$$y_i^{(k+1)} = \text{shrink}(D_\alpha s_i^{(k+1)} + u_i^{(k)}/\rho, \lambda/\rho), \tag{9}$$

where the shrinkage function $\text{shrink}(\cdot,\cdot)$ is defined by

$$\text{shrink}(v, \mu) = (|v| - \mu)_+ \, \text{sgn}(v),$$

where $(x)_+$ is x when $x > 0$, otherwise 0. Here $\text{sgn}(\cdot)$ is the componentwise sign function. The algorithm based on ADMM for solving (4) is summarized in Algorithm 1.

Despite its effectiveness, Algorithm 1 is sensitive to the initialization and returns undesirable solutions numerically-either too sparse using the ℓ_1-regularized solution as initial guess or too diffuse using $\mathbf{0}$ as initial guess. To address this issue, we propose a two-stage algorithm based on ADMM and Geolocation-based Solution Expansion (GSE), termed as Algorithm 2, which is empirically shown to be effective in reconstructing large source extents. At the first stage, we run Algorithm 1 with a small graph parameter β to reduce the impact of misleading (initial) solutions from samples of the same class. Here the solution from the homotopy algorithm [29] is set as the initial guess of S. Although Algorithm 1 locates the most desirable source patches and deactivates the wrongly activated sources, the result is prone to have either narrow or flat source extents. To further correct source extents, we perform GSE, i.e., triggering the neighboring sources of

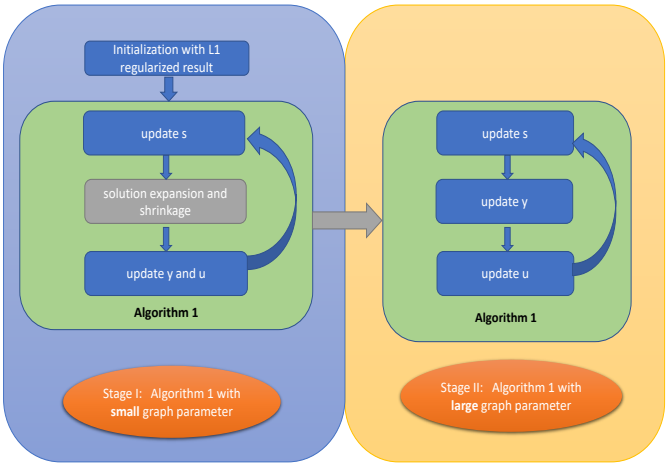

Fig. 1. Pipeline of Algorithm 2

ℓ_1 inferred activated sources to give an overestimation at the first few iterations, followed with expanding the solution by finding a large patch of the source extent. An illustration of the effect of GSE is given in Fig.2. Then the second stage runs Algorithm 1 with a larger β, which corrects the first stage result by eliminating spurious activated sources. Both stages use Algorithm 1 but with different temporal graph parameters and different initial guesses of S.

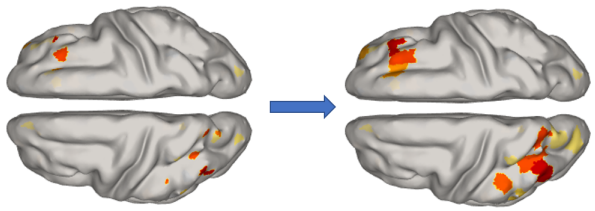

Fig. 2. Illustration of using GSE to expand sparse discrete solution and produce an over-estimated solution. GSE is done by assigning neighbor voxels the same value as the inferred activated sources.

V. Numerical Experiment

A realistic head model called "New York Head" [30] is used in our numerical experiment. The lead field matrix is a linear mapping from 2004 sources to 108 electrodes. We use two focal source extents to represent the spontaneous activation pattern shared by different classes and discriminative task-related pattern corresponding to one brain state. To mimic the real world source propagation pattern, one focal source extent is generated with a center source location and neighboring sources with spatial standard deviation along the cortical manifold with $\sigma = 20$ mm. The magnitude of spontaneous center source is 0.8 and the magnitude of task-related center source is 0.5. Both source extents have 15 activated sources by setting other smaller sources to be 0. We also assign 10 randomly selected source with magnitude of 0.35 with variance to be 0.05 to represent spurious sources for each sample. The maximum iteration is set 50 for updating s_i at each stage. We set $\beta = 10^{-5}$ for the first stage and $\beta = 0.1$

for the second stage. The spatial graph parameter λ is set 10^{-4} to make the data fitting term and the spatial regularization in the same scale. For the GSE operation, we choose 15 sources with largest magnitude, and then assign 5 nearest neighbor sources of them to have the same magnitude starting from the minimum to the largest magnitude of these 15 sources. Fig.2 illustrates the effect under the aforementioned setting. The ground truth source activation and reconstructed sources images as well as a brief discussion by different algorithms are summarized in Fig.3. In Fig.3, the superiority of the proposed two-stage algorithm over sLORETA, MCE, one-stage Algorithm 1 is clearly demonstrated for reconstructing source extents.

For quantitative comparison, we use several metrics including the data fitting r^2, the spatial regularization term R_s defined in (4) to measure the spatial smoothness, predicted source precision P= TP/(TP+FP) and sensitivity S=TP/(TP+FN), where TP, FN, FP represents true positive, false negative and false positive respectively. Note that if the predicted source extent has no overlap with the true source extent, both precision and sensitivity is 0. Here P_c and S_c represent precision and sensitivity for the common source, respectively, and P_d and S_d are defined similarly for the discriminative source. We use threshold values 0.35 and 0.25 when calculating sensitivity and accuracy for the common and the discriminative sources for Homotopy, one-stage Algorithm 1 and two-stage Algorithm 2. We also use the mean absolute error (MAE) to measure the discrepancy between the reconstructed source and the ground truth. Table 1 summarizes the performance of our proposed algorithm and benchmark algorithms. Since Homotopy and one-stage Algorithm 1 without the GSE operation yield very sparse solutions, their precision is high but with very low sensitivity. sLORETA has higher sensitivity accuracy than precision due to its diffusiveness. Our proposed method achieves a better balance of precision and sensitivity. Despite of its capability to better explain the data and a smaller spatial regularization term than the proposed result, the result by one-stage Algorithm 1 is very focalized with narrow source extent. The proposed Algorithm 2 corrects the source extent and provides a more useful result in practice.

Table 1. Performance Comparison

Algorithm	r^2	R_s	P_c	S_c	P_d	S_d	MAE
sLORETA	0.503	487.7	0.27	0.33	0.14	0.7	84.9
Homotopy	1.000	244.5	0.70	0.19	0.72	0.23	20.0
Algorithm 1	0.979	209.5	0.64	0.20	0.62	0.23	18.6
Algorithm 2	0.976	229.2	0.77	0.54	0.82	0.93	16.8

VI. Conclusion

It is a challenging problem to locate the extended source patches due to the high coherence of lead field matrix. In this work, we propose a novel EEG source imaging model using the spatial graph fractional-order TV and the temporal graph regularization involving label information of brain state. The model is solved efficiently by an ADMM-based algorithm. To further correct source extents, a two-stage algorithm is proposed to combine geolocation-based solution expansion. Numerical experiments have demonstrated that the proposed method can preserve high-order spatial smoothness and intra-class consistency, which shows the great potential to achieve high resolution EEG source localization for real-time non-invasive brain imaging research.

References

[1] C. Lamus, M. S. Hämäläinen, S. Temereanca, E. N. Brown, and P. L. Purdon, "A spatiotemporal dynamic solution to the meg inverse problem: An empirical bayes approach," *arXiv preprint arXiv:1511.05056*, 2015.

[2] C. M. Michel, M. M. Murray, G. Lantz, S. Gonzalez, L. Spinelli, and R. G. de Peralta, "EEG source imaging," *Clinical neurophysiology*, vol. 115, no. 10, pp. 2195–2222, 2004.

[3] S. Haufe, V. V. Nikulin, A. Ziehe, K.-R. Müller, and G. Nolte, "Combining sparsity and rotational invariance in EEG/MEG source reconstruction," *NeuroImage*, vol. 42, no. 2, pp. 726–738, 2008.

[4] M. S. Hämäläinen and R. J. Ilmoniemi, "Interpreting magnetic fields of the brain: minimum norm estimates," *Medical & biological engineering & computing*, vol. 32, no. 1, pp. 35–42, 1994.

[5] K. Uutela, M. Hämäläinen, and E. Somersalo, "Visualization of magnetoencephalographic data using minimum current estimates," *NeuroImage*, vol. 10, no. 2, pp. 173–180, 1999.

[6] R. D. Pascual-Marqui *et al.*, "Standardized low-resolution brain electromagnetic tomography (sloreta): technical details," *Methods Find Exp Clin Pharmacol*, vol. 24, no. Suppl D, pp. 5–12, 2002.

[7] Y. Li, J. Qin, Y.-L. Hsin, S. Osher, and W. Liu, "s-SMOOTH: Sparsity and smoothness enhanced EEG brain tomography," *Frontiers in Neuroscience*, vol. 10, p. 543, 2016.

[8] L. Ding, "Reconstructing cortical current density by exploring sparseness in the transform domain," *Physics in Medicine and Biology*, vol. 54, no. 9, p. 2683, 2009.

[9] Y. Li, J. Qin, S. Osher, and W. Liu, "Graph Fractional-Order Total Variation EEG Source Reconstruction," in *2016 38th Annual International Conference of the IEEE Engineering in Medicine and Biology Society (EMBC)*, Orlando, Florida, August 2016, pp. 101–104.

[10] J. Qin, T. Wu, Y. Li, W. Yin, and W. Osher, S.and Liu, "Accelerated High-resolution EEG Source Imaging," in *8th International IEEE EMBS Conference on Neural Engineering (NER' 17)*, Shanghai, China, May 2017.

[11] A. Gramfort, M. Kowalski, and M. Hämäläinen, "Mixed-norm estimates for the M/EEG inverse problem using accelerated gradient methods," *Physics in medicine and biology*, vol. 57, no. 7, p. 1937, 2012.

[12] A. Gramfort, D. Strohmeier, J. Haueisen, M. S. Hämäläinen, and M. Kowalski, "Time-frequency mixed-norm estimates: Sparse M/EEG imaging with non-stationary source activations," *NeuroImage*, vol. 70, pp. 410–422, 2013.

[13] F. Liu, R. Hosseini, J. Rosenberger, S. Wang, and J. Su, "Supervised discriminative EEG brain source imaging with graph regularization," in *International Conference on Medical Image Computing and Computer-Assisted Intervention (MICCAI) (in press)*. Springer, 2017.

[14] F. Liu, J. Rosenberger, Y. Lou, R. Hosseini, J. Su, and S. Wang, "Graph regularized EEG source imaging with in-class consistency and out-classdiscrimination," *IEEE Transactions on Big Data (in press)*.

[15] F. Liu, S. Wang, J. Rosenberger, J. Su, and H. Liu, "A sparse dictionary learning framework to discover discriminative source activations in EEG brain mapping." in *AAAI*, 2017, pp. 1431–1437.

[16] Z. Ren, C. He, and Q. Zhang, "Fractional order total variation regularization for image super-resolution," *Signal Processing*, vol. 93, no. 9, pp. 2408–2421, 2013.

[17] D. Chen, S. Sun, C. Zhang, Y. Chen, and D. Xue, "Fractional-order TV-L2 model for image denoising," *Central European Journal of Physics*, vol. 11, no. 10, pp. 1414–1422, 2013.

[18] J. Bai and X. Feng, "Fractional-order anisotropic diffusion for image denoising," *Image Processing, IEEE Transactions on*, vol. 16, no. 10, pp. 2492–2502, 2007.

[19] K. B. Oldham and J. Spanier, *The Fractional Calculus*. New York: Academic Press, 1974.

[20] H. Guo, Z. Jiang, and L. S. Davis, "Discriminative dictionary learning with pairwise constraints," in *Asian Conference on Computer Vision*. Springer, 2012, pp. 328–342.

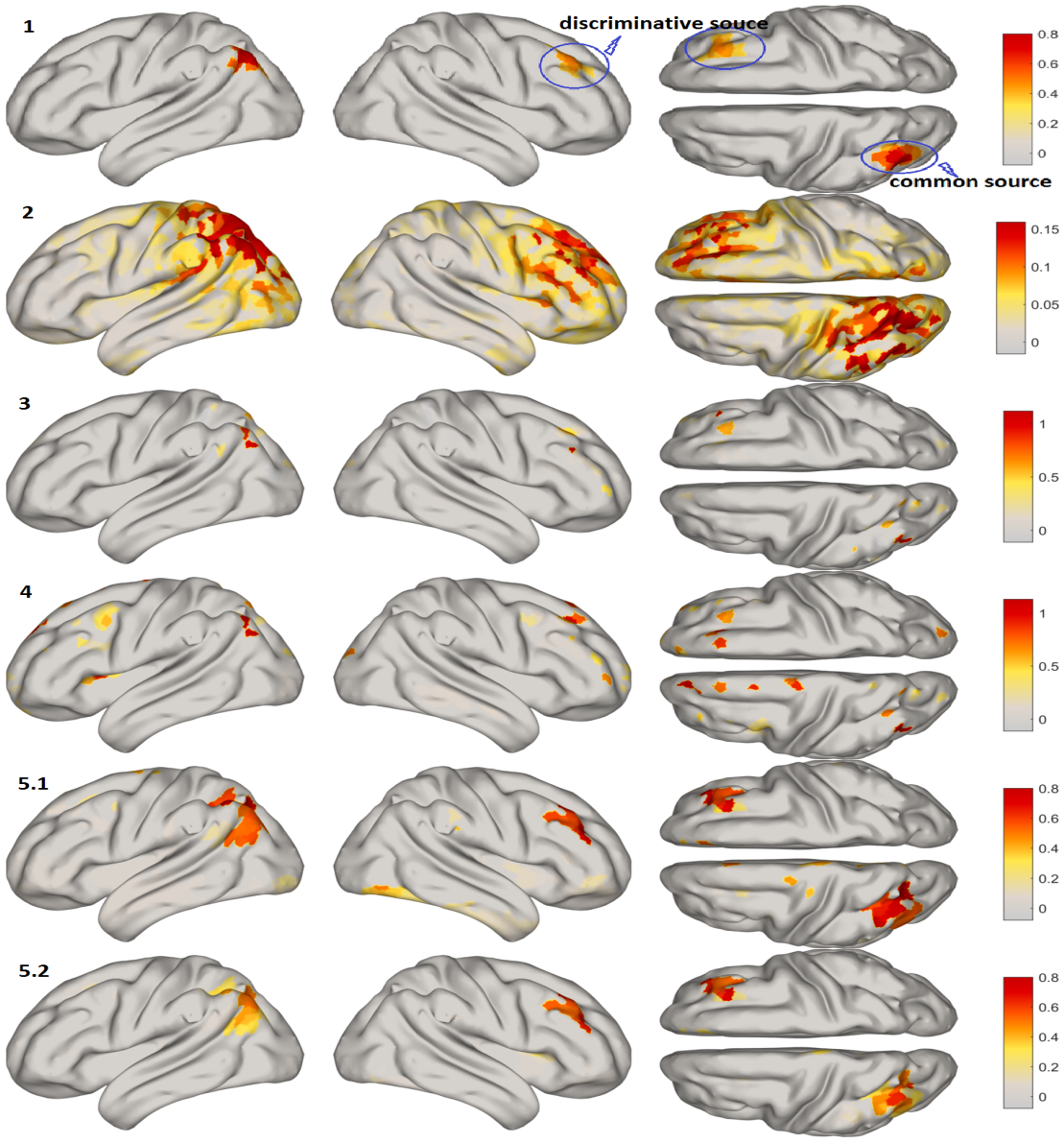

Fig. 3. Ground truth source activation and reconstructed sources by difference algorithms. The top row is ground truth activation pattern. The 2nd row is the sLORETA solution, the 3rd row is the ℓ_1-regularized solution based on the Homotopy algorithm, the 4th row is the one-stage Algorithm 1 solution without GSE, and the row denoted as 5.1 is the solution after the first stage of the proposed algorithm, the row denoted as 5.2 is our final proposed solution. The sLORETA gives over-diffuse and inaccurate solution. Algorithm 1 with the ℓ_1-regularized solution as initial guess gives a very sparse solution. The proposed two-stage algorithm produces the best solution, where spurious activated sources at the first stage are eliminated at the second stage.

[21] M. Zhu, W. Zhang, D. L. Dickens, and L. Ding, "Reconstructing spatially extended brain sources via enforcing multiple transform sparseness," *NeuroImage*, vol. 86, pp. 280–293, 2014.

[22] J. F. Hipp, D. J. Hawellek, M. Corbetta, M. Siegel, and A. K. Engel, "Large-scale cortical correlation structure of spontaneous oscillatory activity," *Nature neuroscience*, vol. 15, no. 6, pp. 884–890, 2012.

[23] M. E. Raichle, "The brain's dark energy," *Science*, vol. 314, no. 5803, pp. 1249–1250, 2006.

[24] H. Liu, P. H. Schimpf, G. Dong, X. Gao, F. Yang, and S. Gao, "Standardized shrinking LORETA-FOCUSS (SSLOFO): a new algorithm for spatio-temporal EEG source reconstruction," *IEEE Transactions on Biomedical Engineering*, vol. 52, no. 10, pp. 1681–1691, 2005.

[25] C. Lamus, M. S. Hämäläinen, S. Temereanca, E. N. Brown, and P. L. Purdon, "A spatiotemporal dynamic distributed solution to the meg inverse problem," *NeuroImage*, vol. 63, no. 2, pp. 894–909, 2012.

[26] S. Castaño-Candamil, J. Höhne, J.-D. Martínez-Vargas, X.-W. An, G. Castellanos-Domínguez, and S. Haufe, "Solving the EEG inverse problem based on space–time–frequency structured sparsity constraints," *NeuroImage*, vol. 118, pp. 598–612, 2015.

[27] D. Strohmeier, Y. Bekhti, J. Haueisen, and A. Gramfort, "The iterative reweighted mixed-norm estimate for spatio-temporal MEG/EEG source reconstruction," *IEEE transactions on medical imaging*, vol. 35, no. 10, pp. 2218–2228, 2016.

[28] S. Boyd, N. Parikh, E. Chu, B. Peleato, and J. Eckstein, "Distributed optimization and statistical learning via the alternating direction method of multipliers," *Foundations and Trends in Machine Learning*, vol. 3, no. 1, pp. 1–122, 2011.

[29] A. Y. Yang, S. S. Sastry, A. Ganesh, and Y. Ma, "Fast ℓ 1-minimization algorithms and an application in robust face recognition: A review," in *Image Processing (ICIP), 2010 17th IEEE International Conference on*. IEEE, 2010, pp. 1849–1852.

[30] S. Haufe and A. Ewald, "A simulation framework for benchmarking EEG-based brain connectivity estimation methodologies," *Brain topography*, pp. 1–18, 2016.